



Assessment of transient elastography in diagnosing MAFLD and the early effects of sleeve gastrectomy on MAFLD among the Chinese population

Ruixiang Hu, MD^{a,b}, Bing Wu, MD^{a,b}, Cunchuan Wang, MD^{a,b}, Zilong Wu, MD^{a,b}, Xu Zhang, MB^d, Xinxin Chen, MD^c, Guanhua Lu, MD^{a,b,c,*}, Kaisheng Yuan, MD^{a,b,*}

Background: Metabolic dysfunction-associated fatty liver disease (MAFLD) has become a prevalent chronic liver disease among patients with obesity. Bariatric surgery, such as sleeve gastrectomy (SG), shows promise in improving the unfavorable condition of MAFLD. Transient elastography (TE) can be utilized to assess the extent of steatosis and liver fibrosis, providing a noninvasive method for preoperative prediction and postoperative evaluation of MAFLD. This study aims to investigate the effectiveness of TE in diagnosing MAFLD by evaluating liver steatosis and tissue stiffness, as well as assessing the early impact of SG in the treatment of obesity-associated MAFLD.

Methods: In this study, the authors collected preoperative and 6-month postoperative data from patients with obesity who were diagnosed with MAFLD by intraoperative liver biopsy. The patients underwent SG at our hospital between August 2021 and April 2023. The authors estimated the diagnostic accuracy for the steatosis and fibrosis categories using the area under the receiver operating characteristic curve (AUROC). The authors also evaluated the influence of disease prevalence on the positive predictive value and negative predictive value. MAFLD diagnosis was based on the liver steatosis activity and fibrosis scoring system. The authors used univariate and multivariate logistic regression analyses to identify factors contributing to severe MAFLD. To visualize the results, the authors created a nomogram and enhanced it with bootstrap resampling for internal validation. Additionally, the authors plotted receiver operating characteristic and calibration curves. The authors compared preoperative and postoperative data, including general information, laboratory tests, and TE results, to assess the early impact of SG in the treatment of obesity-associated MAFLD.

Results: Based on the results of liver biopsy, the AUROC for controlled attenuation parameter (CAP) in identifying steatosis was found to be 0.843 (95% CI: 0.729–0.957) for $S \geq S1$, 0.863 (95% CI: 0.786–0.940) for $S \geq S2$, and 0.872 (95% CI: 0.810–0.934) for $S = S3$. The Youden limits for $S \geq S1$, $S \geq S2$, and $S \geq S3$ were determined to be 271 dB/m, 292 dB/m, and 301 dB/m, respectively. Similarly, the AUROC for liver stiffness measurement (LSM)/E in detecting liver fibrosis was 0.927 (95% CI: 0.869–0.984) for $F \geq F2$, 0.919 (95% CI: 0.824–0.979) for $F \geq F3$, and 0.949 (95% CI: 0.861–0.982) for $F = F4$, with Youden cutoff values of 7.5 kPa, 8.3 kPa, and 10.4 kPa, respectively. Patients with $A \geq 3$ and/or $F \geq 3$ were classified as having severe MAFLD. Multivariate logistic regression analysis identified CAP, E, LDL, and AST as the best diagnostic factors for severe MAFLD, and a nomogram was constructed based on these factors. The AUROC of the nomogram for the assessment of severe MAFLD was 0.824 (95% CI: 0.761–0.887), which was further validated by 1000 bootstrap resamplings with a bootstrap model area under curve of 0.823. Finally, after a 6-month follow-up period, the steatosis grade and fibrosis stage of the patients were graded based on the optimal cutoff values for CAP and LSM. Significant reductions in BMI, waist circumference, HbA1c, fasting glycemia, triglycerides, high density lipoprotein (HDL), glutamic pyruvic transaminase (ALT), glutamic oxaloacetic transaminase (AST), gamma glutamyl transpeptidase (GGT), CAP, LSM, steatosis grade, and fibrosis stage were observed compared to the preoperative values.

Conclusion: In this prospective study, the authors investigated the use of CAP and LSM as alternatives to liver biopsy for evaluating hepatic steatosis and fibrosis in patients with obesity combined with MAFLD. Furthermore, the authors examined the impact of SG on metabolic indicators and the progression of fatty liver disease during the early postoperative period, and observed significant improvements in both aspects.

Keywords: metabolic dysfunction-associated fatty liver disease, nomogram, obesity, sleeve gastrectomy, transient elastography

^aDepartment of Metabolic and Bariatric Surgery, The First Affiliated Hospital of Jinan University, ^bGuangdong-Hong Kong-Macao Joint University Laboratory of Metabolic and Molecular Medicine, The University of Hong Kong and Jinan University, ^cDepartment of Breast Surgery, The Second Affiliated Hospital of Guangzhou Medical University, Guangzhou, Guangdong Province and ^dHarbin Medical University, Harbin 150028, Heilongjiang Province, People's Republic of China

Ruixiang Hu and Bing Wu contributed equally to this work and share the first authorship.

Sponsorships or competing interests that may be relevant to content are disclosed at the end of this article.

*Corresponding author. Address: Department of Metabolic and Bariatric Surgery, The First Affiliated Hospital of Jinan University, No. 613, Huangpu Avenue West, Guangzhou, Guangdong Province 510630, China. Tel.: +86 15818103452. E-mail: 15818103452@163.com (G. Lu), and Tel.: +86 15223342358. E-mail: yuan_kaisheng@163.com (K. Yuan).

Copyright © 2024 The Author(s). Published by Wolters Kluwer Health, Inc. This is an open access article distributed under the terms of the Creative Commons Attribution-Non Commercial-No Derivatives License 4.0 (CCBY-NC-ND), where it is permissible to download and share the work provided it is properly cited. The work cannot be changed in any way or used commercially without permission from the journal.

International Journal of Surgery (2024) 110:2044–2054

Received 28 November 2023; Accepted 27 December 2023

Published online 11 January 2024

<http://dx.doi.org/10.1097/JS9.0000000000001078>

Introduction

As a metabolic disease, obesity is often accompanied by a range of diseases such as diabetes, ischemic heart disease, chronic kidney disease, fatty liver, sleep apnea, hypertension, and various cancers, significantly contribute to mortality. Nonalcoholic fatty liver disease (NAFLD) has emerged as the most prevalent chronic liver condition globally, affecting a quarter of the global population^[1].

NAFLD is closely associated with components of metabolic syndrome, including insulin resistance, diabetes, dyslipidemia, and obesity^[2]. In 2020, an international expert consensus introduced the concept of metabolic dysfunction-associated fatty liver disease (MAFLD) as a rebranding of NAFLD. This rebranding emphasizes the potential metabolic dysregulation features that accompany MAFLD, including dyslipidemia, insulin resistance, elevated blood pressure, and obesity^[3].

Liver biopsy is considered the gold standard for diagnosing MAFLD, but it is an invasive and challenging procedure, making it unsuitable for large-scale research populations^[4]. Current noninvasive diagnostic methods for MAFLD mainly rely on MRI, which is time-consuming and costly^[5]. Consequently, it is impractical as a routine diagnostic approach for MAFLD. Furthermore, ultrasound imaging alone provides limited parameters and is susceptible to interference from fat, resulting in low sensitivity and specificity^[6]. Therefore, it is not suitable as a noninvasive diagnostic approach for MAFLD. Other imaging diagnostic measures also have suboptimal performance.

In the field of noninvasive diagnosis of MAFLD, researchers have introduced a new parameter called the controlled attenuation parameter (CAP) to assess hepatic steatosis without invasive procedures. CAP employs a vibration-controlled transient elastography (TE) method to measure the ultrasound attenuation caused by liver fat^[7]. This technique involves emitting shear waves through a vibrating probe axis that propagate within the patient's body. The ultrasound transducer on the probe emits ultrasound waves to track the propagation and measure its speed, which is then displayed as corresponding images on the monitor. The FibroScan device, a noninvasive diagnostic tool, is specifically designed for liver TE. It is known for its simplicity, rapidity, ease of operation, repeatability, cost-effectiveness, safety, and tolerability^[8]. The device effectively assesses the severity of liver fibrosis and steatosis, showing great potential for widespread application. CAP quantifies the degree of ultrasound signal attenuation in the liver, providing a quantitative diagnosis of hepatic steatosis by reflecting liver fat content. On the other hand, liver stiffness measurement (LSM) can to some extent indicate the degree of liver fibrosis, making it useful for quantitatively detecting liver hardness and steatosis^[9]. When dealing with obese patients, using an XL probe instead of an M probe is more likely to yield reliable measurements^[10].

Multiple prospective studies have indicated^[11–13] that bariatric surgery (BS) can improve metabolic syndrome and reduce MAFLD scoring. It can also mitigate its pathological features, such as reducing steatohepatitis and liver fibrosis. The beneficial effects of BS on MAFLD are long-lasting. Accurate preoperative prediction of MAFLD status is advantageous for clinicians and patients when making surgical and nonsurgical intervention decisions. Similarly, effective postoperative assessment of MAFLD status helps clinicians and patients understand the postoperative remission rate of MAFLD, enabling targeted interventions. Both preoperative prediction and postoperative assessment of MAFLD status are crucial for personalized or precision treatment.

HIGHLIGHTS

- Controlled attenuation parameter and liver stiffness measurement detected by FibroScan can quantitatively diagnose the degree of hepatic steatosis and hepatic fibrosis in metabolic dysfunction-associated fatty liver disease with high sensitivity and specificity.
- The nomogram model has been developed for diagnosing severe metabolic dysfunction-associated fatty liver disease.
- Sleeve gastrectomy could improve metabolic indicators and the status of fatty liver disease during the early postoperative period.

In this prospective study, we applied inclusion and exclusion criteria to select patients undergoing BS. We performed preoperative liver TE and compared the results with the pathological diagnosis from routine liver biopsies. The aim was to examine the concordance between liver TE and liver biopsy, and to investigate the effectiveness of noninvasive TE imaging in predicting MAFLD before surgery. Additionally, we developed a predictive model for severe MAFLD and created a nomogram. After the surgery, the patients were followed up at 6 months and underwent liver TE to assess the early therapeutic effects of sleeve gastrectomy (SG) on obese patients with MAFLD.

Methods

Patients' selection

This study included obese patients (BMI ≥ 28 kg/m²) diagnosed with MAFLD following liver biopsy during SG at our hospital from August 2021 to April 2023. The diagnostic criteria for MAFLD were based on the 2020 'The Asian Pacific Association for the Study of the Liver clinical practice guidelines for the diagnosis and management of metabolic associated fatty liver disease'^[14]. These criteria required evidence of fatty liver on imaging (ultrasound/CT/MR) or $> 5\%$ hepatic steatosis on biopsy, along with one of the following: BMI ≥ 23.0 kg/m², type 2 diabetes (T2D), or metabolic dysfunction. The study adhered to the 1975 Declaration of Helsinki and received approval from the Institutional Review Board of our hospital. All participants provided written informed consent. This study has been registered in the Chinese Clinical Trials Registry. The protocol has been reported in line with the strengthening the reporting of cohort, cross-sectional and case-control studies in surgery (STROCSS) criteria^[15].

Inclusion and exclusion criteria

In this study, the inclusion criteria for patients were as follows: 1. Patients with a BMI of ≥ 35 kg/m², regardless of presence, absence, or severity of comorbidities, and for whom BS did not pose excessive risk; or 2. Patients with a BMI of ≥ 30 – 34.9 kg/m² and one or more severe obesity-related complications that could be corrected by BS^[16]. 3. Patients aged 18–65 years who were willing to participate in the study. 4. Patients who agreed to undergo routine intraoperative liver biopsy and had a valid pathological diagnosis of MAFLD. On the other hand, the exclusion criteria were: 1. Patients incapable of performing daily living activities. 2. Pregnant or breastfeeding patients. 3. Patients with severe preoperative liver or kidney dysfunction, cardiopulmonary failure, or

other serious medical conditions. 4. Patients with a history of severe psychiatric or psychological disorders. 5. Patients in the active phase of cancer.

At the 6-month mark after BS, professional follow-up nurses collected patient information and conducted follow-up visits at the hospital. With patient consent, free liver TE was performed, along with health education and guidance.

Patient characteristics

Demographic information for the patients was collected, which included age, sex, BMI, waist circumference, alcohol consumption, presence of hypertension, diabetes, hyperlipidemia, and hyperuricemia. Alcohol abuse was defined as an average alcohol intake of ≥ 20 g/d for females and ≥ 30 g/d for males. Prior to SG and at the 6-month follow-up, patients underwent a 12 h fast. Serological test data were collected, including glycemic indicators (HbA1c, fasting glycemia), lipid metabolism indicators (cholesterol, triglycerides, high density lipoprotein (HDL), low density lipoprotein (LDL)), liver function (glutamic pyruvic transaminase (ALT), glutamic oxaloacetic transaminase (AST), gamma glutamyl transpeptidase (GGT),

serum albumin), and kidney function (creatinine (Cr), uric acid (UA)), among others.

TE

CAP and LSM measurements were conducted by certified operators within 3 days prior to SG and again at the 6-month postsurgery. Prior to the examination, all patients fasted for at least 3 hours. The patients were positioned in a supine position with full exposure of the thoracoabdominal area, and the right hand was placed behind the head to expand the intercostal space. The detection area ranged from the right 7th to the 9th intercostal spaces, extending from the anterior axillary line to the mid-axillary line. B-mode ultrasound was used for precise positioning, avoiding cysts, large vessels, nodules, and ribs, while ensuring a uniform liver parenchyma within 8.5 cm below the probe centerline. At least 10 valid measurements were performed for each patient, with a total detection rate of $\geq 60\%$ ^[17]. The results were expressed as medians, with an interquartile range to median ratio (IQR/M) $\leq 30\%$ ^[17]. The CAP and LSM measurements (LSM) were recorded using the FibroScan 502 device from Echosens, France, with all probes being of the XL type.

Table 1
Characteristics of patients with and without severe MAFLD based on liver histology.

| Variable | Total | Nonsevere MAFLD | Severe MAFLD | P |
|---|---|---|------------------------------------|----------------|
| Number of patients | 160 | 60 | 100 | |
| Age at surgery (year) | 32.22 \pm 9.21 | 33.03 \pm 8.91 | 31.74 \pm 9.39 | 0.393 |
| Sex n (%) | | | | 0.273 |
| Male | 51 (31.87%) | 16 (26.67%) | 35 (35%) | |
| Female | 109 (68.12%) | 44 (73.33%) | 65 (65%) | |
| BMI (kg/m ²) | 39.37 \pm 7.22 | 37.36 \pm 5.34 | 40.58 \pm 7.93 | 0.003 |
| Waist circumference (cm) | 119.46 \pm 16.29 | 116.44 \pm 12.54 | 121.27 \pm 17.99 | 0.048 |
| HbA1c (%) | 6.29 \pm 1.47 | 6.23 \pm 1.54 | 6.33 \pm 1.43 | 0.694 |
| Fasting glycemia (g/l) | 6.56 \pm 2.07 | 6.41 \pm 1.97 | 6.65 \pm 2.12 | 0.479 |
| Cholesterol (mmol/l) | 5.33 \pm 1 | 5.32 \pm 1.08 | 5.33 \pm 0.95 | 0.994 |
| Triglycerides (mmol/l) | 2 \pm 2.45 | 2.19 \pm 3.27 | 1.88 \pm 1.79 | 0.432 |
| HDL (mmol/l) | 1.1 \pm 0.24 | 1.13 \pm 0.22 | 1.08 \pm 0.25 | 0.188 |
| LDL (mmol/l) | 3.15 \pm 0.63 | 2.87 \pm 0.53 | 3.31 \pm 0.63 | < 0.001 |
| ALT (U/l) | 63.96 \pm 36.91 | 51.57 \pm 33.88 | 71.39 \pm 36.81 | 0.001 |
| AST (U/l) | 48.4 \pm 22.63 | 37.65 \pm 24.21 | 54.85 \pm 19.01 | < 0.001 |
| GGT (U/l) | 51.64 \pm 43.69 | 55.93 \pm 49.5 | 49.07 \pm 39.84 | 0.338 |
| Cr (μ mol/l) | 59.25 \pm 15.08 | 59.42 \pm 12.65 | 59.15 \pm 16.42 | 0.913 |
| Serum albumin (g/l) | 42.77 \pm 3.37 | 42.73 \pm 3.66 | 42.79 \pm 3.21 | 0.918 |
| UA (μ mol/l) | 416.3 \pm 120.64 | 402.91 \pm 117.88 | 424.33 \pm 122.14 | 0.278 |
| Length of liver specimen (mm) ¹ | 18.76 \pm 6.03 | 16.42 \pm 5.41 | 20.17 \pm 5.96 | < 0.001 |
| Steatosis grade (0/1/2/3) ¹ | 15/17/35/93 (9.38%/10.62%/21.88%/58.13%) | 5/8/14/33 (8.33%/13.33%/23.33%/55%) | 10/9/21/60 (10%/9%/21%/60%) | 0.794 |
| Ballooning grade (0/1/2) ¹ | 3/123/34 (1.88%/76.88%/21.25%) | 0/56/4 (0/93.33%/6.67%) | 3/67/30 (3%/67%/30%) | 0.001 |
| Lobular inflammation grade (0/1/2/3) ¹ | 9/71/73/7 (5.62%/44.38%/45.62%/4.38%) | 9/51/0/0 (15%/85%/0/0) | 0/20/73/7 (0/20%/73%/7%) | < 0.001 |
| Fibrosis stage (0/1/2/3/4) ¹ | 59/54/24/4/19 (36.88%/33.75%/15%/2.5%/11.88%) | 25/25/10/0/0 (41.67%/41.67%/16.67%/0/0) | 34/29/14/4/19 (34%/29%/14%/4%/19%) | 0.003 |
| CAP (dB/m) | 313.14 \pm 41.14 | 293.35 \pm 30.83 | 325.02 \pm 42.09 | < 0.001 |
| E (kPa) | 7.81 \pm 4.99 | 5.53 \pm 1.34 | 9.17 \pm 5.82 | < 0.001 |
| Hypertension n (%) | 19 (11.88%) | 6 (10%) | 13 (13%) | 0.570 |
| Diabetes n (%) | 19 (11.88%) | 4 (6.67%) | 15 (15%) | 0.115 |
| Hyperlipemia n (%) | 30 (18.75%) | 8 (13.33%) | 22 (22%) | 0.174 |
| Hyperuricemia n (%) | 32 (20%) | 10 (16.67%) | 22 (22%) | 0.414 |
| Alcohol abuse n (%) | 38 (23.75%) | 12 (20%) | 26 (26%) | 0.388 |

1. based on liver histology.

Values of $P < 0.05$ were bolded. Continuous variables in this paper were normally distributed and expressed as mean \pm SD. Comparisons between groups were made using the independent samples *t*-test. Categorical variables were expressed as frequencies (*n*) and percentages (%), and the χ^2 test was used to compare between groups.

ALT, alanine transaminase; AST, aspartate transaminase; Cr, creatinine; GGT, gamma glutamyl transpeptidase; HDL, high density lipoprotein; LDL, low density lipoprotein; UA, uric acid.

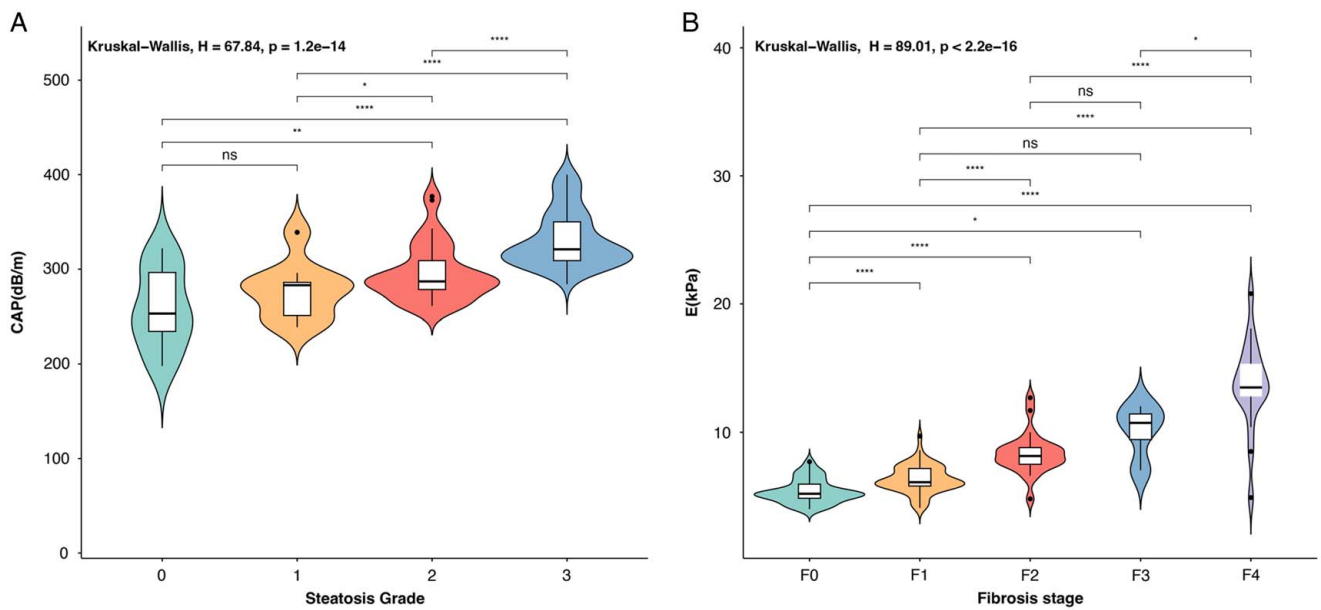


Figure 1. Boxplot of (A) controlled attenuation parameter vs steatosis grade, (B) liver stiffness measurement vs fibrosis stage.

Liver histopathology

Histopathological diagnosis of all liver tissue samples was conducted by experienced pathologists who were unaware of the LSM and CAP results. The nonalcoholic steatohepatitis (NASH) Clinical Research Network Pathology Committee’s (NASH-CRN) NAS grading system was used to score for steatosis (0 to 3), ballooning (0 to 2), lobular inflammation (0 to 3), fibrosis (0 to 4), and NAFLD activity score. Severe MAFLD was defined as active A ≥ 3 and/or fibrosis F ≥ 3^[18].

Statistical analysis

Statistical analysis was performed using SPSS 26.0 (Chicago, IL, USA). The χ^2 test was utilized to compare count data between groups, which were reported as frequencies (*n*) and percentages (%). Measurement data were expressed as mean ± SD and compared between groups using the grouped *t*-test. To assess differences in CAP and LSM across grades of steatosis and stages of fibrosis, the Kruskal–Wallis test was employed, followed by post-hoc comparisons using the Dunn test. Statistical significance was defined as a *P*-value < 0.05. Liver biopsy pathology results were considered the ‘gold standard’ for determining the optimal diagnostic thresholds for CAP and LSM, and corresponding receiver operating characteristic (ROC) curves were plotted. Sensitivity (Se), specificity (Sp), positive predictive value (PPV), negative predictive value (NPV), positive likelihood ratio (LR+) and negative likelihood ratio (LR-) were reported for each cutoff value.

Patients’ MAFLD status was diagnosed using the liver steatosis activity and fibrosis scoring system. R language software and related packages were utilized to select significant variables through univariate logistic regression analysis for inclusion in multivariate logistic regression analysis to identify the best diagnostic factors. A nomogram diagnostic model was constructed, and ROC curves were plotted to calculate the area under the

curve (AUC). The model was internally validated using the enhanced Bootstrap method, and calibration curves were used to demonstrate calibration. General data, laboratory tests, and TE measurements at 6 months post-SG were compared with pre-operative data to evaluate the early effects of SG in treating obesity combined with MAFLD. *P* < 0.05 was considered statistically significant.

Results

Patient characteristics

The study cohort consisted of 160 patients who underwent SG at our hospital from August 2021 to April 2023. These patients

| Table 2 | | | |
|--|--------------------------------|---------------------------------|---------------------------------|
| Diagnostic performance of CAP for S ≥ S1, S ≥ S2, and S = S3. | | | |
| | S ≥ S1 (≥ 5% steatosis) | S ≥ S2 (≥ 34% steatosis) | S = S3 (≥ 67% steatosis) |
| Prevalence (<i>n</i>) | 91.63% (<i>n</i> = 145) | 80% (<i>n</i> = 128) | 58.13% (<i>n</i> = 93) |
| AUROC (95% CI) | 0.843 (0.729–0.957) | 0.863 (0.786–0.940) | 0.872 (0.810–0.934) |
| Youden index | | | |
| Cutoff (dB/m) | 271 | 292 | 301 |
| Se | 0.91 | 0.83 | 0.95 |
| Sp | 0.67 | 0.79 | 0.76 |
| PPV | 0.96 | 0.94 | 0.85 |
| NPV | 0.43 | 0.53 | 0.91 |
| FP | 5 | 7 | 16 |
| FN | 13 | 22 | 5 |
| LR+ | 2.73 | 3.79 | 3.96 |
| LR- | 0.13 | 0.22 | 0.07 |

FN, number of false negative; FP, number of false positive; LP-, negative likelihood ratio; LR+, positive likelihood ratio; NPV, negative predictive value; PPV, positive predictive value; S, steatosis; Se, sensitivity; Sp, specificity.

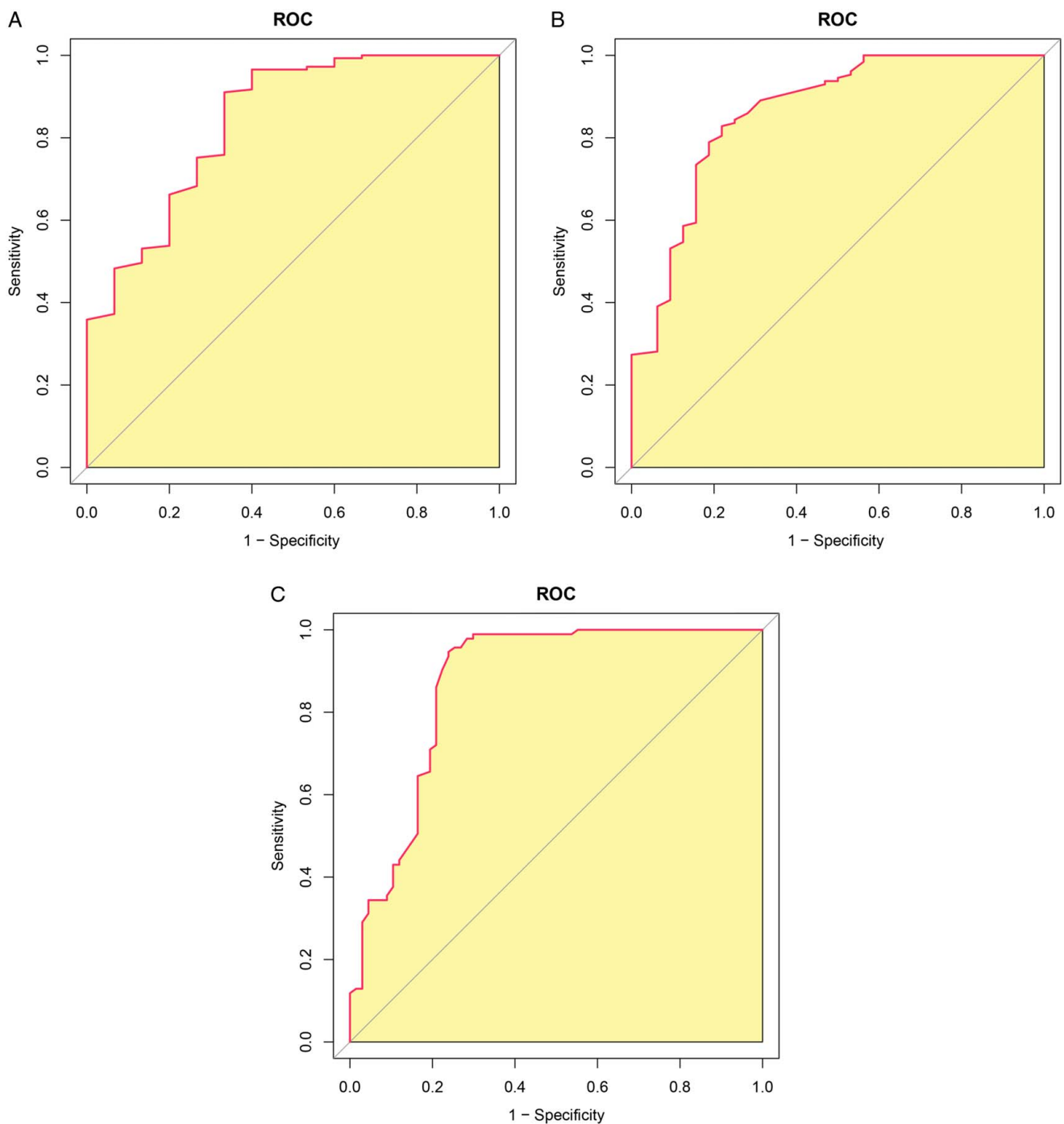


Figure 2. Receiver operating characteristic curve of controlled attenuation parameter for identifying (a) $S \geq S1$, (b) $S \geq S2$, and (c) $S = S3$.

were diagnosed with MAFLD based on liver biopsies performed during surgery. Data collection involved gathering medical history, conducting physical examinations, performing biochemical assessments, conducting effective FibroScan evaluations, and following up with patients 6 months after surgery. Patient demographics are summarized in Table 1. The average age of the study population was 32.22 ± 9.21 years, with males accounting for 31.87%. The average BMI was 39.37 ± 7.22 kg/m², and the mean waist circumference was 119.46 ± 16.29 cm.

Assessment of steatosis using CAP

Based on the results of liver pathology, the distribution of steatosis grades was as follows: $S0 = 15$ (9.38%), $S1 = 17$ (10.62%), $S2 = 35$ (21.88%), $S3 = 93$ (58.13%). The box plot in Figure 1A illustrates the relationship between CAP values and steatosis grade. It is evident that CAP values increase as liver steatosis progresses. Significant differences were observed between all groups except $S0$ and $S1$ (Kruskal–Wallis $H = 67.84$, $P = 1.2 \times 10^{-14}$). The symbols

‘****’, ‘***’, ‘**’, ‘*’, and ‘ns’ represent ‘ $P < 0.0001$ ’, ‘ $P < 0.001$ ’, ‘ $P < 0.01$ ’, ‘ $P < 0.05$ ’, and ‘no significance’, respectively. Table 2 provides detailed diagnostic performance metrics. Under the threshold for $S \geq S1$, the area under the receiver operating characteristic curve (AUROC) was 0.843 (95% CI: 0.729–0.957), with a sensitivity of 0.91 and specificity of 0.67. This threshold was determined as 271 dB/m by maximizing the Youden’s index. For the $S \geq S2$ threshold, the AUROC was 0.863 (0.786–0.940) with a sensitivity of 0.83 and specificity of 0.78, and the threshold was 292 dB/m. The $S \geq S3$ threshold had the highest accuracy, with an AUROC of 0.872 (0.810–0.934), a sensitivity of 0.95, and specificity of 0.76, and the threshold was 301 dB/m. These thresholds were also determined by maximizing the Youden’s index. Figure 2A–C show the ROC curves for $S \geq S1$, $S \geq S2$, and $S = S3$.

Assessment of fibrosis using LSM

The distribution of fibrosis stages was as follows: F0 = 59 (36.88%), F1 = 54 (33.75%), F2 = 24 (15%), F3 = 4 (2.5%), F4 = 19 (11.88%). The box plot in Figure 1B illustrates the LSM values against fibrosis stage. It is evident that LSM values increase as liver steatosis progresses. Significant differences were observed among all groups except F1 and F3, and F2 and F3 (Kruskal–Wallis $H = 89.01$, $P < 2.2 \times 10^{-16}$). Detailed diagnostic performance metrics are provided in Table 3. For the threshold of $F \geq F2$, the AUROC was 0.927 (95% CI: 0.869–0.984), with a sensitivity of 0.89 and specificity of 0.92, and the threshold was 7.5 kPa. The AUROC decreased to 0.919 (0.824–0.979) for the $F \geq F3$ threshold, with a sensitivity of 0.91 and specificity of 0.90, and the threshold was 8.5 kPa. The $F \geq F4$ threshold had the highest accuracy, with an AUROC of 0.949 (0.861–0.982), a sensitivity of 0.89, and specificity of 0.99, and the threshold was 10.4 kPa. These thresholds were determined by maximizing the Youden’s index. The ROC curves for $F \geq F2$, $F \geq F3$, and $F = F4$ are shown in Figure 3A–C.

Univariate and multivariate logistic regression analysis for severe MAFLD

Patients who had $A \geq 3$ and/or $F \geq 3$ on liver biopsy were categorized as having severe MAFLD, resulting in 129 cases of nonsevere MAFLD and 60 cases of severe MAFLD. Significant differences were observed between the two groups in terms of BMI, waist circumference, LDL, ALT, AST, length of liver specimen, ballooning grade, lobular inflammation, and fibrosis stage (all $P < 0.05$). Furthermore, the results of FibroScan showed statistically significant differences between the two groups, with CAP and LSM demonstrating variations ($P < 0.001$) (Table 1).

The results of both univariate and multivariate logistic regression analyses, presented in Table 4, aimed to assess the relationship between variables and severe MAFLD. The univariate logistic regression analysis revealed that BMI, LDL, ALT, AST, length of liver specimen, CAP, and LSM were statistically significant ($P < 0.05$). In the multivariate logistic regression, LDL, AST, CAP, and LSM were identified as the most effective diagnostic factors for predicting severe MAFLD ($P < 0.05$). The multivariate model also explored all possible two-way interactions between variables, but no statistically significant interactions were found ($P > 0.05$).

Table 3
Diagnostic performance of LSM for $F \geq F2$, $F \geq F3$, and $F = F4$.

| | $F \geq F2$ | $F \geq F3$ | $F = F4$ |
|----------------|-------------------------------|-------------------------------|----------------------------|
| Prevalence (n) | 29.38% (n = 47) | 14.38% (n = 23) | 11.88% (n = 19) |
| AUROC (95% CI) | 0.927 (0.869–0.984) | 0.919 (0.824–0.979) | 0.949 (0.861–0.982) |
| Youden index | | | |
| Cutoff (kPa) | 7.5 | 8.3 | 10.4 |
| Se | 0.89 | 0.91 | 0.89 |
| Sp | 0.92 | 0.90 | 0.99 |
| PPV | 0.82 | 0.60 | 0.89 |
| NPV | 0.95 | 0.98 | 0.99 |
| FP | 9 | 14 | 2 |
| FN | 5 | 2 | 2 |
| LR + | 11.22 | 8.93 | 63.08 |
| LR- | 0.12 | 0.14 | 0.11 |

F, fibrosis; FN, number of false negative; FP, number of false positive; LP-, negative likelihood ratio; LR +, positive likelihood ratio; NPV, negative predictive value; PPV, positive predictive value; Se, sensitivity; Sp, specificity.

Construction and internal validation of the diagnostic model for severe MAFLD

A multivariate logistic regression analysis was conducted to develop a diagnostic model for severe MAFLD. The model included LDL, AST, CAP, LSM, and their corresponding weight coefficients. The analysis was performed using the R software. The results were visually represented in a nomograph (Fig. 4) and ROC curves were generated. The nomo model achieved an AUC of 0.824 (95% CI: 0.761–0.887) for diagnosing severe MAFLD, with a sensitivity of 0.90 and specificity of 0.61, indicating excellent discriminative ability (Fig. 5A). To assess the model’s performance further, the enhanced Bootstrap method was used for internal validation. The model development dataset was resampled 1000 times with replacement, resulting in 1000 datasets of equal sample size. The Bootstrap model yielded an AUC of 0.823, indicating robust discriminative performance even after internal validation (Fig. 5B). A calibration curve was plotted (Fig. 5C), which showed an average absolute error of 0.032 between the predicted probabilities and actual probabilities. The Hosmer–Lemeshow test indicated no statistically significant differences ($P = 0.420$), suggesting excellent calibration of the nomo model and a high level of agreement between diagnostic probabilities and actual probabilities. Furthermore, when considering high-risk thresholds ranging from 0.25 to 0.75, the net benefit remained greater than zero, signifying clinical significance. Notably, as the high-risk threshold decreased, the net benefit increased, indicating improved clinical utility (Fig. 5D).

Comparison of basic conditions before and 6 months after SG

Postoperative 6-month patients’ steatosis and fibrosis were staged using the optimal cutoff values for CAP and LSM obtained earlier. The distribution was as follows: for steatosis, S0 = 127 (79.38%), S1 = 20 (12.50%), S2 = 3 (1.88%), and S3 = 10 (6.25%); for fibrosis, F0-1 = 137 (85.63%), F2 = 5 (3.13%), F3 = 11 (6.88%), and F4 = 7 (4.38%). A comparative analysis between preoperative and postoperative 6-month data was then conducted, encompassing general information, laboratory assessments, and TE measurements. The results revealed statistically significant reductions in BMI, waist circumference,

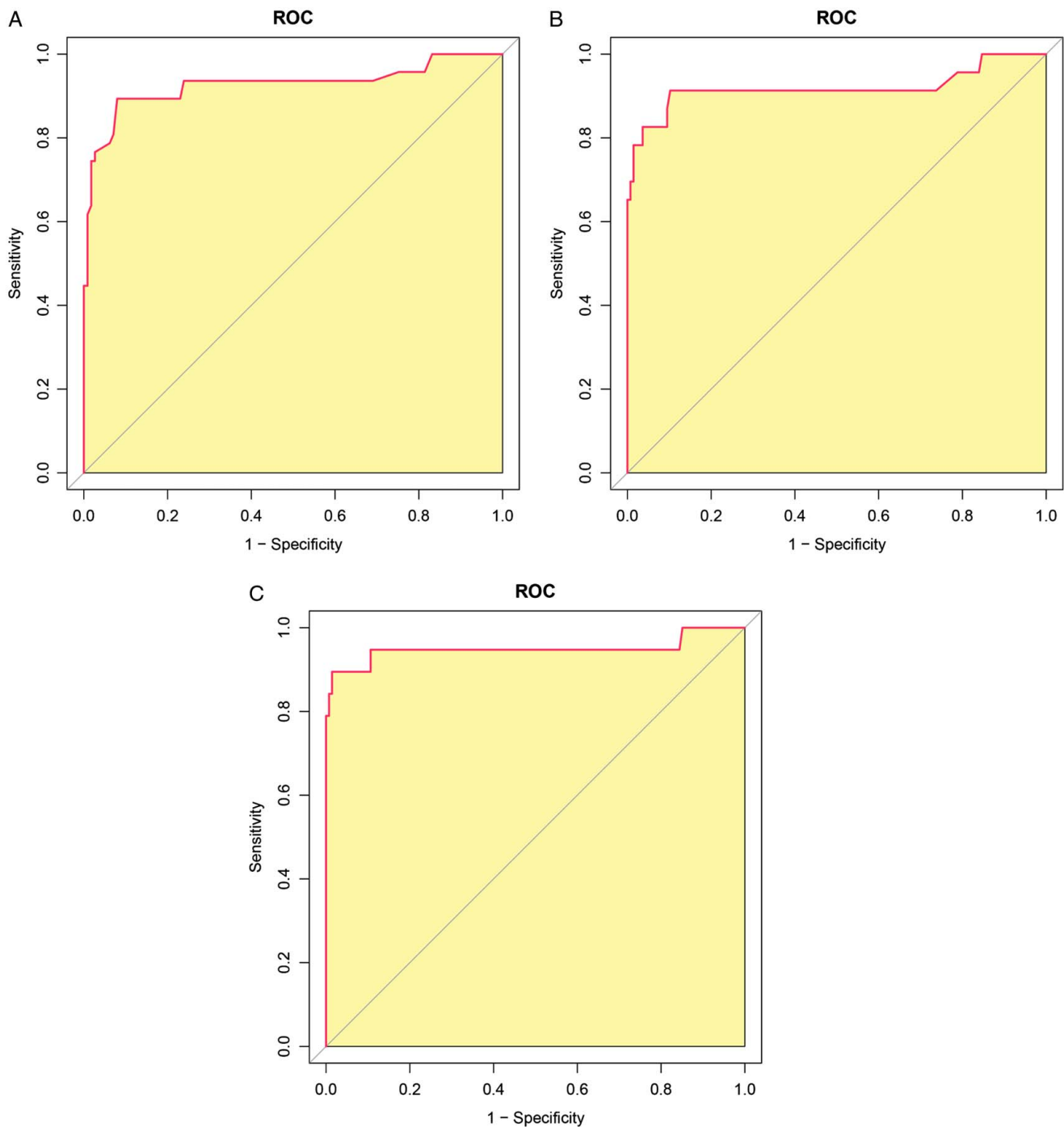


Figure 3. Receiver operating characteristic curve of liver stiffness measurement for identifying (a) $F \geq F2$, (b) $F \geq F3$, and (c) $F = F4$.

HbA1c, fasting glycemia, triglycerides, HDL, ALT, AST, GGT, CAP, LSM, Steatosis grade, and Fibrosis stage compared to preoperative values ($P < 0.001$) (Table 5).

Discussion

Obesity has become a global epidemic, often accompanied by various diseases such as insulin resistance, T2D, MAFLD, NASH,

hypertension, cardiovascular diseases, and certain cancers^[19]. In the past decade, the prevalence of MAFLD has been increasing, in line with the rise in obesity rates. This may be attributed to the increased flow of free fatty acids to the liver in patients with obesity, resulting in liver damage^[19]. Early diagnosis and treatment of MAFLD are crucial in preventing further progression, considering its potential reversibility.

Currently, liver biopsy and imaging are internationally recognized as the standard methods for diagnosing fatty liver.

Table 4
Univariate and multivariate logistic regression analyses of variables associated with the presence of severe MAFLD based on liver histology.

| Variables | Univariate analysis | | Multivariate analysis | |
|--------------------------|---------------------|----------------|-----------------------|--------------|
| | OR (95% CI) | P | OR (95% CI) | P |
| Age at surgery (year) | | | | |
| Sex | | | | |
| Female | Reference | 0.275 | | |
| Male | 1.48 (0.73–3) | | | |
| BMI | 1.08 (1.02–1.13) | 0.008 | 1 (0.93–1.07) | 0.907 |
| Waist circumference | 1.02 (1–1.04) | 0.071 | | |
| HbA1c | 1.05 (0.84–1.31) | 0.692 | | |
| Fasting glycemia | 1.06 (0.9–1.25) | 0.478 | | |
| Cholesterol | 1 (0.73–1.38) | 0.994 | | |
| Triglycerides | 0.95 (0.83–1.08) | 0.448 | | |
| HDL | 0.41 (0.11–1.55) | 0.189 | | |
| LDL | 3.62 (1.94–6.75) | < 0.001 | 2.77 (1.36–5.62) | 0.005 |
| ALT | 1.02 (1.01–1.03) | 0.002 | 0.99 (0.97–1.01) | 0.219 |
| AST | 1.05 (1.03–1.07) | < 0.001 | 1.02 (1–1.04) | 0.040 |
| GGT | 1 (0.99–1) | 0.338 | | |
| Cr | 1 (0.98–1.02) | 0.913 | | |
| Serum albumin | 1.01 (0.91–1.11) | 0.915 | | |
| UA | 1 (1–1) | 0.277 | | |
| Length of liver specimen | 1.13 (1.06–1.2) | < 0.001 | 1.02 (0.93–1.12) | 0.721 |
| CAP | 1.02 (1.01–1.03) | < 0.001 | 1.01 (1–1.02) | 0.043 |
| LSM | 1.59 (1.26–1.99) | < 0.001 | 1.39 (1.08–1.81) | 0.012 |
| Hypertension | | | | |
| No/Unknown | Reference | | | |
| Yes | 1.34 (0.48–3.75) | 0.571 | | |
| Diabetes | | | | |
| No/Unknown | Reference | | | |
| Yes | 2.47 (0.78–7.83) | 0.124 | | |
| Hyperlipidemia | | | | |
| No/Unknown | Reference | | | |
| Yes | 1.83 (0.76–4.43) | 0.178 | | |
| Hyperuricemia | | | | |
| No/Unknown | Reference | | | |
| Yes | 1.41 (0.62–3.23) | 0.416 | | |
| Alcohol abuse | | | | |
| No/Unknown | Reference | | | |
| Yes | 1.41 (0.65–3.05) | 0.389 | | |

Values of *P* < 0.05 were bolded. ALT, alanine transaminase; AST, aspartate transaminase; Cr, creatinine; GGT, gamma glutamyl transpeptidase; HDL, high density lipoprotein; LDL, low density lipoprotein; OR, odds ratio; UA, uric acid.

While liver biopsy is considered the ‘gold standard’ for clinical diagnosis of fatty liver diseases, it has limitations such as high-risk, cost, invasiveness, and unsuitability for repeated screening, which makes it less acceptable to a wide range of patients^[20–22]. Therefore, there is an urgent need for a non-invasive diagnostic method to replace liver biopsy. A recent device called FibroScan offers a new quantitative method for diagnosing MAFLD. It is noninvasive, cost-effective, rapid, operator-independent, radiation-free, repeatable, and has broad clinical application prospects^[23]. Several studies^[20,24,25] have found FibroScan to be highly sensitive and specific for MAFLD, demonstrating high diagnostic accuracy.

To date, no prospective study has investigated the histological characteristics and diagnostic accuracy of FibroScan in assessing MAFLD in Chinese populations with morbid obesity. The XL probe of FibroScan has been shown to decrease the failure rate of

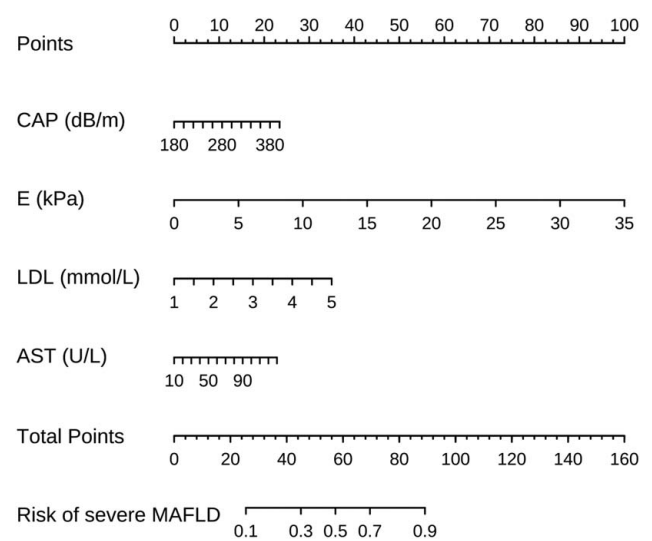


Figure 4. Nomogram of the predicted probability of severe metabolic dysfunction-associated fatty liver disease.

LSM and unreliable results in patients with obesity^[26]. In a study of 193 consecutive NAFLD patients undergoing liver biopsy and paired LSM, Wong and colleagues found that the XL probe was more likely to achieve 10 valid measurements (95 vs 81%; *P* < 0.001) and a success rate over 60% (90 vs 74%; *P* < 0.001) compared to the M probe^[10]. Therefore, this study chose the XL probe of FibroScan to assess and grade MAFLD in Chinese populations with morbid obesity and MAFLD for the first time, providing a theoretical basis for selecting noninvasive diagnostic and treatment methods in the clinical differentiation and determination of MAFLD.

The results of this study indicate that the sensitivity and specificity for ≥ S1, ≥ S2, and S3 were 0.91 and 0.67, 0.83 and 0.78, and 0.95 and 0.76, respectively. The optimal cutoff values for diagnosing S1, S2, and S3 using CAP were 271 dB/m, 292 dB/m, and 301 dB/m, respectively. Similarly, for ≥ F2, ≥ F3, and F4, the sensitivity and specificity were 0.89 and 0.92, 0.91 and 0.90, and 0.89 and 0.99, respectively. The optimal cutoff values for diagnosing F2, F3, and F4 using LSM were 7.5 kPa, 8.5 kPa, and 10.4 kPa, respectively. These findings suggest that FibroScan, which measures CAP and LSM, can provide quantitative assessments of fatty changes and liver fibrosis with good diagnostic efficacy. This makes it a valuable tool in clinical settings for early diagnosis and quantification of MAFLD. FibroScan can also help assess disease progression and develop appropriate treatment plans for patients to control disease progression. However, it is important to note that the cutoff values derived from this study may not align entirely with those from other studies^[27]. This discrepancy could be attributed to the single-center nature of this study and the limited sample size. Therefore, further validation is necessary to assess the diagnostic value and determine appropriate thresholds.

As MAFLD progresses, it can develop into NASH, cirrhosis, and then HCC. However, about 20–30% of NAFLD-related HCC occurs without cirrhosis, suggesting that NAFLD-induced HCC has a unique molecular pathogenesis^[28]. Currently, there is

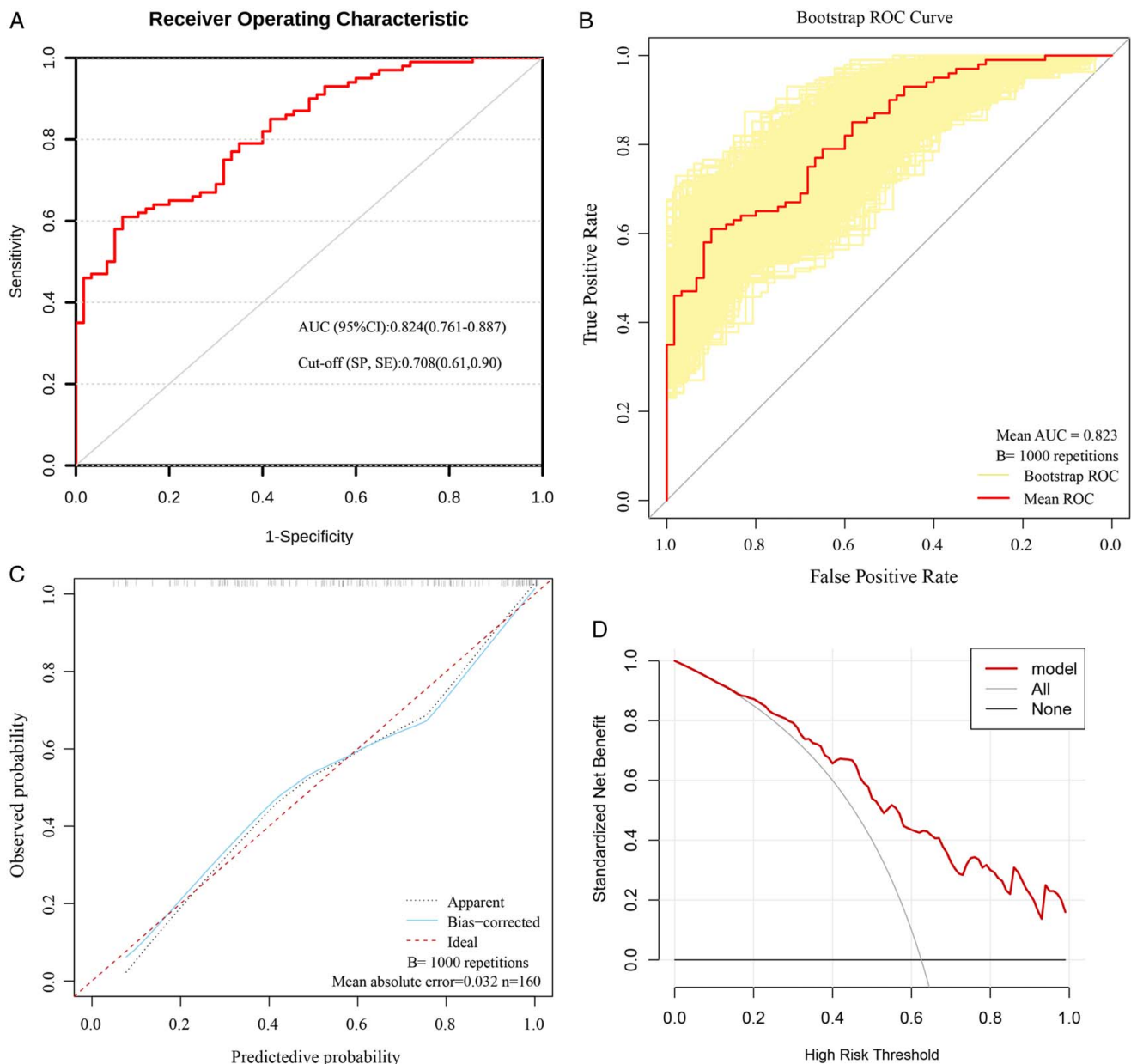


Figure 5. Performance assessment of the predictive model was conducted.

no single marker available for accurately distinguishing severe MAFLD. Therefore, it is necessary to explore accurate and reliable noninvasive diagnostic models. In this study, we established a nomogram model based on LDL, AST, CAP, and LSM for diagnosing severe MAFLD. Both calibration and DCA curves confirmed the good predictive value of the nomogram model.

For patients who are unable to achieve satisfactory weight loss through medication and lifestyle changes, particularly those with obesity and MAFLD, weight loss surgery is the most effective option. The impact of SG on NAFLD has been receiving increasing attention in recent years, with ongoing research in this area^[29,30]. This study involved 160 patients who underwent SG for obesity and MAFLD, aiming to investigate the specific therapeutic effects of SG on MAFLD. By comparing biochemical

indicators and fatty liver conditions before and 6 months after surgery, it was observed that CAP decreased from 313.14 ± 41.14 dB/m before surgery to 236.89 ± 45.9 dB/m after surgery, and LSM decreased from 7.81 ± 4.99 kPa before surgery to 5.32 ± 3.37 kPa after surgery. Optimal cutoff values obtained for CAP and LSM were used to stage postoperative patients for fatty degeneration and fibrosis. Comparison with preoperative stages revealed that S3 decreased from 109 (68.13%) before surgery to 10 (6.25%) after surgery, and F4 decreased from 25 (15.63%) before surgery to 7 (4.38%) after surgery. These findings suggest that LSG has a significant therapeutic effect on patients with obesity and MAFLD.

The design of our study was multifaceted, involving the assessment of the effectiveness of SG on MAFLD and the

Table 5
Comparison of basic conditions before and 6 months after sleeve gastrectomy.

| Variable | Presurgery | 6-month postsurgery | P |
|---|---|---|---------|
| Number of patients | 160 | 160 | |
| BMI (kg/m ²) | 39.37 ± 7.22 | 31.13 ± 6.39 | < 0.001 |
| Waist circumference (cm) | 119.46 ± 16.29 | 100.78 ± 16.08 | < 0.001 |
| HbA1c (%) | 6.29 ± 1.47 | 5.33 ± 0.6 | < 0.001 |
| Fasting glycemia (g/l) | 6.56 ± 2.07 | 5.28 ± 1.04 | < 0.001 |
| Cholesterol (mmol/l) | 5.33 ± 1 | 5.09 ± 1.12 | 0.051 |
| Triglycerides (mmol/l) | 2 ± 2.45 | 1.27 ± 0.52 | < 0.001 |
| HDL (mmol/l) | 1.1 ± 0.24 | 1.21 ± 0.26 | < 0.001 |
| LDL (mmol/l) | 3.15 ± 0.63 | 3 ± 0.85 | 0.087 |
| ALT (U/l) | 63.96 ± 36.91 | 24.58 ± 14.85 | < 0.001 |
| AST (U/l) | 48.4 ± 22.63 | 24.13 ± 11.92 | < 0.001 |
| GGT (U/l) | 51.64 ± 43.69 | 19.2 ± 11.14 | < 0.001 |
| Cr (μmol/l) | 59.25 ± 15.08 | 64.71 ± 40.58 | 0.112 |
| Serum albumin (g/l) | 42.77 ± 3.37 | 43.37 ± 4.46 | 0.178 |
| UA (μmol/l) | 416.3 ± 120.64 | 390.3 ± 120.12 | 0.054 |
| CAP (dB/m) | 313.14 ± 41.14 | 236.89 ± 45.9 | < 0.001 |
| LSM (kPa) | 7.81 ± 4.99 | 5.32 ± 3.37 | < 0.001 |
| Steatosis grade (0/1/2/3) ¹ | 22/23/6/109 (13.75%/14.38%/3.75%/68.13%) | 127/20/3/10 (79.38%/12.50%/1.88%/6.25%) | < 0.001 |
| Fibrosis stage (0-1/2/3/4) ¹ | 107/17/11/25 (66.88%/10.63%/6.88%/15.63%) | 137/5/11/7 (85.63%/3.13%/6.88%/4.38%) | < 0.001 |

1. bases on transient elastography.

Values of $P < 0.05$ were bolded. Continuous variables in this paper were normally distributed and expressed as mean ± SD. Comparisons between groups were made using the independent samples t -test. Categorical variables were expressed as frequencies (n) and percentages (%), and the χ^2 test was used to compare between groups.

ALT, alanine transaminase; AST, aspartate transaminase; Cr, creatinine; GGT, gamma glutamyl transpeptidase; HDL, high density lipoprotein; LDL, low density lipoprotein; UA, uric acid.

development of a new diagnostic model. We chose this approach for two reasons: 1. The SG procedure allowed us to gather comprehensive data, including liver biopsies, which are essential for accurate MAFLD diagnosis. This enabled us to evaluate the impact of SG on MAFLD and investigate the potential of a new diagnostic model simultaneously. 2. Our study was exploratory, aiming to investigate various aspects of MAFLD in the context of BS. By combining these elements, we aimed to maximize the utility of the collected data and explore potential correlations and findings that could inform future, more focused studies.

This study has certain limitations that should be acknowledged. Firstly, the sample size is small and the study was conducted in a single-center, which limits the generalizability of the findings. It provides initial insights but is not sufficient to fully validate the new diagnostic model. Secondly, a meta-analysis has shown that RYGB and SG may be equally efficacious in ameliorating NAFLD^[31], and the exclusion of RYGB patients means that our findings may not be generalizable to all BS types. This limitation is indeed significant, as it restricts our understanding of the comparative effectiveness of different bariatric procedures in the context of MAFLD treatment. Moreover, external validation is lacking, preventing us from assessing how well the model can be applied to other populations. Furthermore, there is a dearth of data from liver pathology biopsies for comparative analysis in the context of weight loss surgery. Therefore, future research endeavors should encompass multicenter studies, include a larger

sample size, and conduct liver biopsies on patients after BS surgery in order to enhance the reliability and validity of the research findings.

Conclusion

This study confirms the applicability of TE in the Chinese population with obesity and MAFLD. Additionally, the nomogram model presented in this study is a preliminary attempt to create a noninvasive diagnostic tool for evaluating severe MAFLD. Although our findings show promise, it is crucial to highlight that this model is still in its early stages and needs to be further validated through a larger study. Furthermore, SG is a safe and effective method for weight reduction. It not only leads to definitive weight loss results but also significantly alleviates MAFLD, while improving liver function and dysregulated lipid metabolism. The short-term (6-month) outcomes are significant and provide new insights into the treatment and improvement of obesity coexisting with MAFLD.

Ethical approval

The study adhered to the 1975 Declaration of Helsinki and received approval from the Institutional Review Board of the First Affiliated Hospital of Jinan University (No.: KY-2022-023). All participants provided written informed consent. This study has been registered in the Chinese Clinical Trials Registry (ChiCTR2100053920).

Consent

Written informed consents were obtained from the patients for publication. A copy of the written consent is available for review by the Editor-in-Chief of this journal on request.

Sources of funding

This study was funded by the Science and Technology Projects in Guangzhou (Funding No.: 202201020063) and the flagship specialty construction project-General surgery of The First Affiliated Hospital of Jinan University (Funding No.: 711003).

Author contribution

R.H. and K.Y.: conceived and designed the main framework of this study; K.Y.: conducted the main data analysis and prepared the manuscript; B.W. and C.W.: were responsible for assisting with data collection and managing the follow-up patients; Z.W. and X.Z.: were tasked with collating as well as analyzing the data; X.C. and G.L.: edited and improved the manuscript. All authors were involved in writing the paper and had final approval of the submitted and published versions.

Conflicts of interest disclosure

The authors state that they have no interests in conflict.

Research registration unique identifying number (UIN)

1. Name of the registry: Transient elastography of the liver for preoperative prediction and postoperative evaluation of bariatric surgery of nonalcoholic fatty liver disease.
2. Unique identifying number or registration ID: ChiCTR2100053920.
3. Hyperlink to your specific registration (must be publicly accessible and will be checked): <https://www.chictr.org.cn/showproj.html?proj=141241>.

Guarantor

As this work's guarantor, Ruixiang Hu has full access to all data in the study and is responsible for the data's integrity and accuracy.

Data availability statement

The data used and analyzed during the current study are available from the corresponding authors on reasonable request.

Provenance and peer review

not commissioned, externally peer reviewed.

References

- [1] Younossi ZM, Koenig AB, Abdelatif D, *et al.* Global epidemiology of nonalcoholic fatty liver disease-Meta-analytic assessment of prevalence, incidence, and outcomes. *Hepatology* 2016;64:73–84.
- [2] Dietrich P, Hellerbrand C. Non-alcoholic fatty liver disease, obesity and the metabolic syndrome. *Best Pract Res Clin Gastroenterol* 2014;28:637–53.
- [3] Eslam M, Newsome PN, Sarin SK, *et al.* A new definition for metabolic dysfunction-associated fatty liver disease: an international expert consensus statement. *J Hepatol* 2020;73:202–9.
- [4] Kwok R, Choi KC, Wong GL, *et al.* Screening diabetic patients for non-alcoholic fatty liver disease with controlled attenuation parameter and liver stiffness measurements: a prospective cohort study. *Gut* 2016;65:1359–68.
- [5] Zhou JH, Cai JJ, She ZG, *et al.* Noninvasive evaluation of nonalcoholic fatty liver disease: current evidence and practice. *World J Gastroenterol* 2019;25:1307–26.
- [6] Pirmoazen AM, Khurana A, El Kaffas A, *et al.* Quantitative ultrasound approaches for diagnosis and monitoring hepatic steatosis in nonalcoholic fatty liver disease. *Theranostics* 2020;10:4277–89.
- [7] Castera L, Vilgrain V, Angulo P. Noninvasive evaluation of NAFLD. *Nat Rev Gastroenterol Hepatol* 2013;10:666–75.
- [8] Castera L, Forns X, Alberti A. Non-invasive evaluation of liver fibrosis using transient elastography. *J Hepatol* 2008;48:835–47.
- [9] Wong VW, Vergniol J, Wong GL, *et al.* Diagnosis of fibrosis and cirrhosis using liver stiffness measurement in nonalcoholic fatty liver disease. *Hepatology* 2010;51:454–62.
- [10] Wong VW, Vergniol J, Wong GL, *et al.* Liver stiffness measurement using XL probe in patients with nonalcoholic fatty liver disease. *Am J Gastroenterol* 2012;107:1862–71.
- [11] Lassailly G, Caiazzo R, Buob D, *et al.* Bariatric surgery reduces features of nonalcoholic steatohepatitis in morbidly obese patients. *Gastroenterology* 2015;149:379–88.
- [12] Lassailly G, Caiazzo R, Ntandja-Wandji LC, *et al.* Bariatric surgery provides long-term resolution of nonalcoholic steatohepatitis and regression of fibrosis. *Gastroenterology* 2020;159:1290–301.e5.
- [13] Bell LN, Temm CJ, Saxena R, *et al.* Bariatric surgery-induced weight loss reduces hepatic lipid peroxidation levels and affects hepatic cytochrome P-450 protein content. *Ann Surg* 2010;251:1041–8.
- [14] Eslam M, Sarin SK, Wong VW, *et al.* The Asian Pacific Association for the Study of the Liver clinical practice guidelines for the diagnosis and management of metabolic associated fatty liver disease. *Hepatol Int* 2020;14:889–919.
- [15] Mathew G, Agha R, Albrecht J, *et al.* STROCCS 2021: strengthening the reporting of cohort, cross-sectional and case-control studies in surgery. *Int J Surg* 2021;96:106165.
- [16] Eisenberg D, Shikora SA, Aarts E, *et al.* 2022 American Society of Metabolic and Bariatric Surgery (ASMBS) and International Federation for the Surgery of Obesity and Metabolic Disorders (IFSO) Indications for Metabolic and Bariatric Surgery. *Obes Surg* 2023;33:3–14.
- [17] Myers RP, Pomier-Layrargues G, Kirsch R, *et al.* Feasibility and diagnostic performance of the FibroScan XL probe for liver stiffness measurement in overweight and obese patients. *Hepatology* 2012;55:199–208.
- [18] Nascimbeni F, Bedossa P, Fedchuk L, *et al.* Clinical validation of the FLIP algorithm and the SAF score in patients with non-alcoholic fatty liver disease. *J Hepatol* 2020;72:828–38.
- [19] Gutiérrez-Cuevas J, Santos A, Armendariz-Borunda J. Pathophysiological molecular mechanisms of obesity: a link between MAFLD and NASH with cardiovascular diseases. *Int J Mol Sci* 2021;22:11629.
- [20] Cheung JTK, Zhang X, Wong GL, *et al.* MAFLD fibrosis score: using routine measures to identify advanced fibrosis in metabolic-associated fatty liver disease. *Aliment Pharmacol Ther* 2023;58:1194–204.
- [21] Carlson JJ, Kowdley KV, Sullivan SD, *et al.* An evaluation of the potential cost-effectiveness of non-invasive testing strategies in the diagnosis of significant liver fibrosis. *J Gastroenterol Hepatol* 2009;24:786–91.
- [22] Stevenson M, Lloyd-Jones M, Morgan MY, *et al.* Non-invasive diagnostic assessment tools for the detection of liver fibrosis in patients with suspected alcohol-related liver disease: a systematic review and economic evaluation. *Health Technol Assess* 2012;16:1–174.
- [23] Huang Z, Ng K, Chen H, *et al.* Validation of controlled attenuation parameter measured by fibroscan as a novel surrogate marker for the evaluation of metabolic derangement. *Front Endocrinol (Lausanne)* 2021;12:739875.
- [24] Tavaglione F, De Vincentis A, Bruni V, *et al.* Accuracy of controlled attenuation parameter for assessing liver steatosis in individuals with morbid obesity before bariatric surgery. *Liver Int* 2022;42:374–83.
- [25] Avcu A, Kaya E, Yilmaz Y. Feasibility of fibroscan in assessment of hepatic steatosis and fibrosis in obese patients: report from a general internal medicine clinic. *Turk J Gastroenterol* 2021;32:466–72.
- [26] Chan WK, Nik Mustapha NR, Wong GL, *et al.* Controlled attenuation parameter using the FibroScan® XL probe for quantification of hepatic steatosis for non-alcoholic fatty liver disease in an Asian population. *United European Gastroenterol J* 2017;5:76–85.
- [27] Karlas T, Petroff D, Sasso M, *et al.* Individual patient data meta-analysis of controlled attenuation parameter (CAP) technology for assessing steatosis. *J Hepatol* 2017;66:1022–30.
- [28] Padilla J, Osman NM, Bissig-Choisat B, *et al.* Circadian dysfunction induces NAFLD-related human liver cancer in a mouse model. *J Hepatol* 2023;S0168-8278:05184.
- [29] Wang G, Wang Y, Bai J, *et al.* Increased plasma genistein after bariatric surgery could promote remission of NAFLD in patients with obesity. *Front Endocrinol (Lausanne)* 2022;13:1024769.
- [30] Zhou H, Luo P, Li P, *et al.* Bariatric surgery improves nonalcoholic fatty liver disease: systematic review and meta-analysis. *Obes Surg* 2022;32:1872–83.
- [31] Baldwin D, Chennakesavalu M, Gangemi A. Systematic review and meta-analysis of Roux-en-Y gastric bypass against laparoscopic sleeve gastrectomy for amelioration of NAFLD using four criteria. *Surg Obes Relat Dis* 2019;15:2123–30.